Published in final edited form as:
Biochem J. ; 424(1): 99–107. doi:10.1042/BJ20090934.

Importance of the bioenergetic reserve capacity in response to cardiomyocyte stress induced by 4-hydroxynonenal

BG Hill[1,*], **BP Dranka**[1,*], **L Zou**[2], **JC Chatham**[2], and **VM Darley-Usmar**[1]

[1] Department of Pathology, Center for Free Radical Biology, University of Alabama at Birmingham, Birmingham, AL 35294-0022

[2] Division of Cardiovascular Disease, Department of Medicine, University of Alabama at Birmingham, Birmingham, AL 35294-0022

SYNOPSIS

Mitochondria play a critical role in mediating the cellular response to oxidants formed during acute and chronic cardiac dysfunction. It is widely assumed that, as cells are subject to stress, mitochondria are capable of drawing upon a “reserve capacity” which is available to serve the increased energy demands for maintenance of organ function, cellular repair, or detoxification of reactive species. This hypothesis further implies that impairment or depletion of this putative reserve capacity ultimately leads to excessive protein damage and cell death. However, it has been difficult to fully evaluate this hypothesis since much of our information about the response of the mitochondrion to oxidative stress derives from studies on mitochondria isolated from their cellular context. Therefore, the goal of this study was to determine whether “bioenergetic reserve capacity” does indeed exist in the intact myocyte and whether it is utilized in response to stress induced by the pathologically relevant reactive lipid species 4-hydroxynonenal (HNE). We found that intact rat neonatal ventricular myocytes exhibit a substantial bioenergetic reserve capacity under basal conditions; however, on exposure to pathologically relevant concentrations of HNE, oxygen consumption was increased until this reserve capacity was depleted. Exhaustion of the reserve capacity by HNE treatment resulted in inhibition of respiration concomitant with protein modification and cell death. These data suggest that oxidized lipids could contribute to myocyte injury by decreasing the bioenergetic reserve capacity. Furthermore, these studies demonstrate the utility of measuring the bioenergetic reserve capacity for assessing or predicting the response of cells to stress.

Keywords

Mitochondria; lipid peroxidation; oxidative stress; glycolysis; extracellular flux; heart

INTRODUCTION

Defining the role of mitochondria in various cardiovascular pathologies is currently an area of great interest, with many studies focusing on the properties of the organelle isolated from diseased or stressed cardiac cells. These studies now point to the importance of understanding how changes in isolated mitochondria translate to changes in bioenergetic events that take place in the myocardium during ischemia-reperfusion and heart failure. Cardiac tissue is rich in mitochondria, which are capable of dynamically responding to energy demand for increased

Corresponding author: Victor M. Darley-Usmar, Ph.D., Department of Pathology, University of Alabama at Birmingham, Biomedical Research Building II, 901 19th Street South, Birmingham, Alabama 35294, Tel: 205-975-9507, Fax: 205-934-7447, darley@uab.edu.
*These authors contributed equally to this work.

work. This oxidative phenotype allows for rapid and substantial ATP production for cardiac function. It is clear from experiments using ^{31}P NMR that, even under an increased work load in the physiological range, mitochondria appear to have a substantial “reserve capacity” which is depleted under conditions of severe stress such as pressure overload or ischemia [1,2]. However, this concept has proved technically difficult to examine using direct indices of mitochondrial function in intact myocytes.

Data from mitochondria isolated from hearts subject to stress typically show changes in the activity of the respiratory chain, but the functional impact remains unclear once the organelles are removed from their cellular context [3,4]. It is frequently the case that the activity of respiratory chain complexes of isolated mitochondria such as complex I are decreased in the diseased heart [5,6]. It is challenging to extend these changes to the cellular setting since the control over metabolism is lost in isolated mitochondria. For example, it is known that the maximal capacity for oxidative phosphorylation is higher than that used under normal conditions [2]. This raises the question of the role of this reserve capacity and leads to the hypothesis that it is required by cells to respond to stress and that pathological events occur when this bioenergetic reserve is depleted.

The requirement of the reserve capacity for the response to stress, such as occurs in the ischemic and failing heart, has not been examined in intact cardiovascular cells or tissues. Since the diseased heart is associated with increased oxidative stress, exposure of cells to reactive species generated during pathology can be used as a model of pathology and to test the role of oxidative stress in myocyte dysfunction. The significance of these reactive species is evidenced by studies showing that overexpression of antioxidant enzymes such as Mn-superoxide dismutase (SOD) [7], catalase [8], extracellular-SOD [9], or glutathione peroxidase [10] protects the heart from ischemia-reperfusion injury. Moreover, partial deficiency of Mn-SOD [11] or the complete absence of glutathione peroxidase [12] or CuZn-SOD [13] renders the heart more sensitive to injury. Interestingly, volume and pressure overload [14–16] as well as ischemia [17,18] result in an increased ability of myocytes to consume oxygen, which might suggest a mechanism for further depletion of the bioenergetic reserve capacity in an environment where oxygen availability may be already limiting.

Secondary products of oxidative stress such as 4-hydroxynonenal (HNE) are normally detoxified by energy requiring processes; however, under pathological conditions, these detoxification pathways fail leading to accumulation of oxidized lipids [19] that can damage key proteins in the mitochondrial respiratory chain. In humans and animal models, downstream products of oxidative stress such as oxidized lipids are abundant in the ischemic [19,20] and failing heart [21,22]. Therefore, the generation of lipid peroxidation products capable of reacting with cellular nucleophiles could be primary instigators of tissue injury [23]. The α,β-unsaturated aldehydes (e.g., HNE) are likely to be the most significant because they modify proteins which affect energy production [24–30] and cell death pathways [31,32]. This is corroborated by studies showing that activation of a key enzyme required for the mitochondrial detoxification of HNE [19] protects the heart from injury [33,34].

These findings raise two important questions: 1) Does bioenergetic reserve capacity exist in cardiac myocytes and 2) Does it modulate the response to stress associated pathology? The recent availability of technology which allows the non-invasive measurement of mitochondrial respiration and glycolysis offers the opportunity to address these questions. Therefore, we hypothesized that maintenance of mitochondrial function and the availability of a bioenergetic reserve capacity is critical to combat oxidative stress and that, when exceeded, protein damage and cell death occurs. To test this hypothesis, we used an emerging technology, high-throughput extracellular flux (XF) analysis, to quantify the bioenergetic changes that occur in intact cardiac myocytes exposed to HNE. By measuring XF, we were able to measure oxygen

consumption and proton production, indicative of oxidative phosphorylation and glycolysis, respectively, in intact rat neonatal ventricular myocytes exposed to HNE.

Our data support the hypothesis that pathologically relevant concentrations of oxidized lipids exhaust the reserve capacity of mitochondria. When this capacity is depleted, cellular injury occurs accompanied by decreased mitochondrial oxygen consumption, decreased efficiency due to proton leak, and increased protein-HNE adduct formation. These results directly demonstrate the presence of a bioenergetic reserve capacity in intact myocytes. Furthermore, these findings suggest that oxidized lipids such as HNE, which accumulate in the heart during ischemia and heart failure, could cause, accelerate, or worsen myocardial injury by diminishing this reserve capacity.

MATERIALS AND METHODS

Materials

Reagent HNE was obtained from Calbiochem (San Diego, CA). All materials and reagents for the Extracellular Flux assays were from Seahorse Biosciences (North Billerica, MA). Nonanal, oligomycin, thiazoyl blue tetrazolium, carbonyl cyanide *p*-[trifluoromethoxy]-phenyl-hydrazone (FCCP), and antimycin A were from Sigma (St. Louis, MO). Secondary HRP-linked antibodies and antibodies against actin were from Cell Signaling (Danvers, MA). Anti-protein HNE antibodies were a gift from Dr. Sanjay Srivastava at the University of Louisville. ECL plus reagents were from GE Healthcare (Pittsburgh, PA).

Neonatal rat ventricular myocyte primary cultures

All animal experiments were approved by the University of Alabama Institutional Animal Care and Use Committee and conformed to the *Guide for the Care and Use of Laboratory Animals*, published by the National Institutes of Health (NIH Publication No. 85-23, Revised 1996). Primary cultures of neonatal rat ventricular myocytes (NRVM) were obtained from 2- to 3-day-old neonatal Sprague-Dawley rats and were cultured as described previously [35]. NRVM were seeded at 75,000 cells/well in collagen-coated Seahorse Bioscience V7 culture plates in growth medium containing 15% fetal bovine serum (FBS) on the first day. On the next day, medium was replaced, and cells were grown in the culture growth medium without FBS. Within 1–2 days of isolation, a confluent monolayer of spontaneously beating NRVM formed, and cells were used as described below.

Bioenergetic measurements

An XF24 Analyzer (Seahorse Biosciences, North Billerica MA) was used to measure bioenergetic function in intact NRVM. The XF24 creates a transient, 7 μl chamber in specialized microplates that allows for oxygen consumption rate (OCR) and extracellular acidification rate (ECAR) or proton production rate (PPR) to be monitored in real time [36]. For all bioenergetic measurements, the culture media was changed 1 h prior to the assay run to unbuffered Dulbecco's Modified Eagle Medium (DMEM, pH 7.4) supplemented with 4 mM L-glutamine (Gibco, Carlsbad, CA). First, the optimum number of cells needed for these experiments was determined. NRVM were seeded to a density of 25,000, 50,000, or 75,000 cells/well. Oxygen consumption in these cells was linear with respect to cell number within this range (Fig. 1A), and a seeding density of 75,000 cells/well was chosen for the remainder of the experiments.

Next, an assay was developed to measure indices of mitochondrial function. Oligomycin, FCCP, and antimycin A were injected sequentially through ports in the Seahorse Flux Pak cartridges to final concentrations of 1 μg/ml, 1 μM, and 10 μM, respectively. This allowed determination of the basal level of oxygen consumption, the amount of oxygen consumption

linked to ATP production, the level of non-ATP linked oxygen consumption (proton leak), the maximal respiration capacity, and the non-mitochondrial oxygen consumption. As shown in Fig. 1B, three basal OCR measurements were recorded prior to injection of oligomycin. After mixing and recording the oligomycin-sensitive OCR, FCCP was injected and another OCR measurement was recorded. The OCR measured after FCCP injection represents the maximal capacity that cells have to reduce oxygen under the experimental conditions. Finally, antimycin A was injected to inhibit the flux of electrons through complex III, and thus no oxygen is further consumed at cytochrome *c* oxidase. The remaining OCR determined after this treatment is primarily non-mitochondrial and could be due to cytosolic oxidase enzymes.

Protein-HNE and GSH measurements

Protein-HNE adducts were detected using a polyclonal anti-protein HNE antibody, as described in [37]. Briefly, cells were lysed in the 24-well XF plates using 20 μl/well of lysis buffer containing 20 mM HEPES, 1 mM DTPA, 1% NP-40, 0.1% SDS, and protease inhibitor cocktail. The lysates were then added to SDS Laemmli Buffer, and the proteins were separated on 10% SDS polyacrylamide gels. After transfer to PVDF membranes, HNE-modified proteins were detected using anti-protein-HNE primary and HRP-linked anti-rabbit secondary antibodies by chemifluorescence on a Typhoon Variable Mode Imager (GE Healthcare, Pittsburgh, PA). Relative levels of protein-HNE adducts were quantified by densitometry using ImageQuantTL software (GE Healthcare, Pittsburgh, PA). Total GSH (GSH+GSSG) was measured in cell lysates with and without treatment with HNE using the Tietze recycling assay [38].

Cell death assays

Cell viability was measured by MTT assay as described previously [39], with the following modifications. NRVM were seeded as described above into V7 culture plates at 75,000 cells/well. At 8 and 16 h after HNE treatment, the assay media was replaced with media containing 0.4 mg/ml thiazoyl blue tetrazolium. The cells were allowed to incubate in a non-CO_2 incubator at 37°C for an additional 2 h. The media was removed, and the resulting formazan crystals were solubilized in 250 μl DMSO. The absorbance was read at 550 nm and the data expressed as a percentage of control.

Statistical analysis

Data are reported as means ± SEM. Comparisons between two groups were performed with unpaired Student's *t*-tests. Comparisons among multiple groups or between two groups at multiple time-points were performed by either one-way or two-way analysis of variance, as appropriate. A p value of less than 0.05 was considered statistically significant.

RESULTS

Protein HNE adducts and cell death increase with HNE treatment

NRVM were seeded at 75,000 cells/well and then treated with either HNE or the non-electrophilic C9 lipid analog of HNE, nonanal, for 2 h. For these experiments, we used concentrations of HNE that have been shown to occur in the ischemic and failing heart [19, 21,40,41]. The cells were harvested and proteins were separated by SDS-PAGE followed by Western blotting with anti-protein-HNE antibodies. As shown in Fig. 2A and B, HNE adducts accumulated in a concentration-dependent manner. The non-protein reactive analog of HNE, nonanal, was used as a structural control and did not promote the formation of protein-HNE adducts. Additionally, cell death as a result of the HNE treatment was examined at 8 and 16 h by the MTT assay. HNE exhibited both a concentration and time dependent effect on NRVM viability (Fig. 2C). HNE can be metabolized by a number of enzymes in the cell including the

glutathione (GSH) dependent S-transferases [19,42]. Accordingly, we measured total GSH (GSH + GSSG) levels in the lysates of cells treated with HNE for 90 min (Fig. 2D). As anticipated HNE treatment depletes GSH and this was maximal at the lowest concentration of HNE tested.

Effect of HNE on aerobic metabolism in intact neonatal cardiomyocytes

To determine if bioenergetic derangements preceded cell death due to HNE, we assessed oxygen consumption in NRVM treated under the same conditions as shown in Fig. 2. After basal oxygen consumption measurements, HNE was injected to give final concentrations of 0–30 μM. Control wells received vehicle (ethanol) or the structural control for HNE, nonanal (10 μM), in DMEM. As shown in Fig. 3A and B, HNE initially increased OCR in a concentration dependent manner. Myocytes treated with the lowest concentration of HNE tested (5 μM) resulted in a steady increase in the rate of mitochondrial oxygen consumption which plateaued after approximately 150 min of HNE exposure. Exposure to higher concentrations of HNE (10–30 μM) resulted in a maximal OCR that declined thereafter. Apparent maximal increases in OCR were reached with 10, 20, and 30 μM HNE approximately 130, 70, and 35 min after injection, respectively. Interestingly, the rate of increase in OCR (i.e., the slope of the initial stimulation of OCR by HNE) increased linearly with HNE concentration (Fig. 3B). Nonanal was used as a structural control for non-electrophilic effects of HNE and did not affect oxygen consumption by the myocytes (data not shown).

To quantify the overall increase in the amount of oxygen consumed by the myocytes due to each treatment, the OCR area under the curve for each group was calculated by multiplying the group average by the time interval for that rate and subtracting the baseline rate. The resulting value can be expressed in pmoles of oxygen consumed during the assay after injection of vehicle, nonanal, or HNE. As shown in Fig. 3C, exposure of the myocytes to HNE at 0–20 μM concentrations resulted in up to approximately 20 nmoles of oxygen consumed during the course of the experiment. The highest concentration of HNE used, i.e., 30 μM, showed no overall increase in oxygen consumption. At this concentration, OCR increased transiently, followed by a rapid decrease in oxygen consumption that was well below baseline (Fig. 3A).

Effects of HNE on glycolysis

In addition to OCR, the XF assay also allowed the measurement of protons that were produced by the cells, which reflects lactate production and is therefore an index of glycolysis [36,43]. Figure 4A shows the extracellular acidification rate (ECAR) profile of control myocytes and myocytes treated with 0–30 μM HNE. Similar to OCR, HNE increased the ECAR in a concentration and time-dependent manner. Analogous to the OCR results (Fig. 3A), ECAR showed a biphasic response in the 10 and 20 μM HNE groups, indicating severe damage to bioenergetic components at later time points. As shown in Fig. 4B, the initial rate of increase in ECAR was linear and dependent on HNE concentration. Similar to that shown for OCR in Fig. 3C, the area under the curve of the proton production rate (PPR) was calculated to determine the overall increase in proton production over the time course of the experiment. HNE treatment resulted in an increase in proton production, indicative of an increase in glycolysis, over the course of the experiment (Fig. 4C). The maximal rate of proton production occurred in cells treated with 7.5–10 μM HNE.

Identification of mitochondrial defects incurred by HNE

Approximately 70 min after HNE addition (indicated by the dotted line in Fig. 5B), the ECAR and OCR were used to obtain a “metabolic image” of the cells in each treatment group. The image is divided in four quadrants, which relate the relative activities of the glycolytic and aerobic metabolism in response to HNE. As shown in Fig. 5A, HNE concentration-dependently

stimulates both glycolysis and the aerobic consumption of oxygen, consistent with an increased energy demand of the cells as they respond to this stress.

To determine the specific mitochondrial derangements that occur in response to HNE, we used the mitochondrial function assay described in Fig 1B. For these experiments, myocytes treated with HNE to final concentrations of 0–20 μM were exposed to oligomycin, FCCP, and antimycin A at the timepoints indicated (Fig. 5B). The measurements taken after each injection were used to calculate the ATP-linked OCR, proton leak, reserve capacity, and non-mitochondrial OCR at 2h after the addition of HNE. As shown in Fig. 6A, OCR was stimulated in response to HNE by 263.1 ± 22.5 pmol/min above the baseline levels. On the addition of oligomycin, Fig 6B shows that the oligomycin-insensitive OCR in the presence of HNE increased significantly by up to 2.5-fold. To determine the individual parameters of mitochondrial function, the data shown in Fig. 5B were analyzed as described in Fig. 1. Proton leak was increased as by HNE in a concentration-dependent manner. Interestingly, the rate of ATP-linked oxygen consumption showed a biphasic response (Fig. 6D), where it increased by approximately 3-fold at the 10 μM HNE and decreased at 20 μM. These results suggest that HNE increases OCR both by increasing proton leak (thereby decreasing mitochondrial efficiency) and by increasing energy demand.

Next, the maximal respiratory rate was determined from the FCCP-stimulated rate. As shown in Fig. 5B, HNE at 0–10 μM concentrations had no effect on this maximal respiratory rate. However, concentrations of HNE in excess of 10 μM resulted in inhibition of oxygen consumption even after FCCP addition, suggesting overt damage to mitochondrial respiratory complexes (Fig. 5B). The reserve capacity was calculated based on the OCR immediately prior to oligomycin addition and the maximal respiratory rate. As shown in Fig. 6E, HNE decreased the mitochondrial reserve capacity in a concentration-dependent manner consistent with damage to the respiratory chain associated with increased protein adducts (Fig. 2A). The rate of oxygen consumption due to non-mitochondrial sources was determined in the presence of HNE using antimycin A and was unchanged (Fig. 5B, 6F).

DISCUSSION

Using extracellular flux analyses, we evaluated the effects of the electrophilic lipid HNE on bioenergetic function in intact myocytes. We show for the first time that oxidized lipids, at concentrations that accumulate under pathophysiological conditions in the heart, increase cardiomyocyte oxygen consumption and deplete the bioenergetic reserve capacity. We found that HNE stimulated the rate of cellular oxygen consumption in a concentration-dependent manner. This increase in oxygen consumption was due to both increased bioenergetic demand placed on the cardiac myocytes and decreased mitochondrial efficiency (i.e., proton leak). Glycolytic flux was also increased in response to HNE treatment, underscoring the integrated nature of the metabolic response to energy demand and expenditure in the presence of reactive lipid species. The HNE-induced increase in oxygen consumption was not compensated by an increase in the maximal respiratory capacity of the myocytes; consequently, HNE treatment resulted in depletion of the bioenergetic reserve capacity, overt respiratory failure, and cell death.

In the heart, mitochondria make up at least 20% of the myocyte volume [44,45] and provide the unremitting energy required for contraction. Aerobic respiration is therefore indispensable to sustain cardiac function and viability. At rest, the heart consumes up to 0.15 ml O_2/min/g tissue, which increases several fold with vigorous exercise by calling upon the reserve capacity of the mitochondria and glycolysis [46]. Interestingly, the diseased heart requires more oxygen to meet energy needs, which has led to the hypothesis that a state of energy starvation may underlie myocardial pathology [47]. In support of this concept, myocardial oxygen uptake is

increased 2-fold in patients with left ventricular hypertrophy over normal subjects [14]; there is also an increase in the myocardial uptake of oxygen in experimental hypertrophy, congestive heart failure, and diabetes [15,16,48]. Furthermore, the postischemic heart uses more oxygen than the preischemic heart [18], and myocytes subjected to hypoxia-reoxygenation have an increased demand for oxygen [17]. It is reasonable to conclude, therefore, that bioenergetic dysfunction and the imbalance of oxygen supply versus demand is a basic defect in myocardial pathologies. However, the mechanisms underlying this increased demand for oxygen in the diseased heart are unknown. Increased tissue levels of reactive species such as HNE are associated with both acute and chronic cardiac disease [19–21,41]. If, as shown here, such reactive species increase the rate of oxygen consumption and bioenergetic reserve capacity in the diseased heart, this could account for the contractile dysfunction associated with pathology.

While the idea that ROS play a fundamental role in cardiovascular disease is well accepted, the molecular mechanisms by which oxidative stress cause cardiac injury are not well defined. ROS can damage cellular components by direct oxidation; however, given the susceptibility of polyunsaturated fatty acids to oxidative attack, there is a strong rationale for invoking the involvement of secondary products of lipid oxidation such as HNE and acrolein in ROS-related injury. Indeed, adducts of such oxidized lipids with proteins have been detected in the diseased heart [19,20,28,30,41,49–51] and myocytes exposed to similar compounds capable of modifying proteins promote a phenotype akin to myocardial stunning [52]. It remains unclear, however, whether oxidized lipids or their protein adducts are footprints of unquenched free radicals or if they indeed cause derangements in signaling or bioenergetics.

Recent studies showing that activation of enzymes critical for HNE detoxification protects the heart from ischemic injury suggest that electrophiles are significant contributors to myocardial damage [33,34]. Many studies have shown that HNE damages electron transport chain complexes [3,25–30], affecting both respiration and critical events such as calcium-induced permeability transition [32,53]. These studies, however, were limited by their usage of isolated mitochondrial preparations. While useful for understanding putative defects caused by HNE, experiments with isolated mitochondria are generally performed under saturating substrate conditions and are outside their normal intracellular environment. This removes all influence of cell signaling, ion fluxes, and changes in intracellular substrate metabolism (e.g., glycolysis) on bioenergetic regulation. In contrast to the HNE-induced increase in oxygen consumption found here, most studies to date report that HNE primarily inhibits mitochondrial respiration. This is likely due to the fact that the majority of studies have assessed HNE-induced changes in respiration using isolated mitochondrial preparations [19,25–27].

Here, we demonstrate that HNE increases oxygen consumption and bioenergetic demand and decreases mitochondrial efficiency (Figs. 3 – 6). These findings suggest that oxidized lipids contribute to myocardial injury by promoting an energy crisis. In support of this concept, we show that HNE at lower concentrations initially increased the OCR (Fig. 3), which was due to both increased proton leak and bioenergetic demand (Fig. 6). Using the process described in Fig. 1 we can assess the impact of HNE on key bioenergetic parameters in the cell. We have assumed for the purposes of this calculation that the oligomycin-insensitive OCR is attributable to proton leak in the basal condition. However, this is not strictly correct since oligomycin has been shown to increase mitochondrial membrane potential and the resulting OCR is likely to be an upper estimate of the contribution from proton leak. While the oligomycin-dependent hyperpolarization has no impact on the conclusion that HNE has increased proton leak (Fig. 6C), it will affect the value of the OCR which we attribute to ATP synthesis primarily through an underestimation of this parameter. Nevertheless, it is clear that a significant portion of the stimulation of the basal OCR was due to increased bioenergetic demand. The increased proton leak across the inner mitochondrial membrane may be mediated by uncoupling proteins or leakage through damaged respiratory complexes. In support of this, studies using isolated

mitochondria have shown that HNE promotes uncoupling and mitochondrial proton leak [24, 54].

The biphasic nature of the HNE-induced changes in oxygen consumption (Figs. 3A and 5B) suggest at least two factors contributing to the effects of HNE. Initially, HNE increased the oxygen consumption rate in a concentration-dependent manner (Fig. 3B). We propose that this is an initial adaptive response to cellular stress induced by HNE and does not involve damage to the respiratory chain. The second phase, where the OCR decreased at the higher concentrations of HNE, is likely due to damage to respiratory complexes. Another possibility is that endogenous substrates became limiting as OCR increased. This is unlikely since 20 and 30 μM HNE, which quickly reached a peak respiratory capacity in the cells (Figs. 3A), resulted in a lower overall consumption of oxygen compared with myocytes treated with 5 and 10 μM HNE (Fig. 3C) and decreased the ability of the cells to respire maximally when treated with the uncoupler, FCCP (Fig. 5B). Furthermore, the concentrations of HNE that caused a transient breach of the reserve capacity (i.e., 10–30 μM HNE) were associated with substantially increased protein-HNE adducts, and this resulted in complete cell death (Fig. 2A and 2B). As anticipated GSH was rapidly depleted by HNE and was maximal at the lowest concentration of HNE tested. Since the major bioenergetic changes induced by HNE occurred without a significant change in these repressed GSH levels it is unlikely that GSH depletion plays a major role in the HNE-dependent bioenergetic dysfunction reported here. From these data, therefore, it is likely that extensive formation of protein-HNE adducts caused damage to respiratory complexes that resulted in inhibition of electron transport.

As discussed above, HNE levels are substantially increased in multiple myocardial pathologies [19–21,41,51], suggesting that HNE promotes tissue damage and dysfunction by decreasing the bioenergetic reserve capacity. Interestingly, myocardial oxygen consumption in the pressure-overloaded heart is increased to the maximal dinitrophenol-stimulated rate during high workloads produced by catecholamine infusion [2], suggesting that reserve capacity is depleted in the diseased heart under conditions of stress. This is particular interesting since even low dose catecholamine treatment promotes lipid peroxidation and the formation of protein-HNE adducts [22,51]. While of particular relevance to cardiovascular disease, reduced bioenergetic reserve capacity has also been recognized in neurodegeneration. Specifically, reduction of the spare respiratory capacity has been shown to regulate glutamate excitotoxicity in neurons [55,56]. Those studies suggested that dysfunction occurs when the ATP demand exceeds the maximal ATP supply put forth by glycolysis and oxidative phosphorylation, thereby implicating the spare respiratory capacity critical for maintaining ATP generation under conditions of increased demand [57]. Similarly, we show that the ability of cardiomyocyte mitochondria to respire collapses when the maximal reserve capacity is depleted due to the increase in oxygen consumption by HNE (Fig. 6C).

Taken as a whole, these data support the view that products of lipid peroxidation, in the concentration range reported under pathological conditions, contribute to myocardial injury by promoting bioenergetic stress. By evaluating mitochondrial function in intact cells, our findings reveal for the first time a dynamic response of cardiomyocytes to HNE, where oxygen consumption is increased through increased energy demand as well as via non-ATP-linked oxygen sinks (i.e., proton leak). Furthermore, these studies provide insight into a fundamental mechanism critical to the evolution of myocyte injury, namely the oxidized lipid-induced increase in oxygen consumption and depletion of the bioenergetic reserve capacity. Consequently, these findings have implications not only for our understanding of the pathophysiological processes underlying cardiac disease, but also in other disease states associated with increased oxidative stress.

Acknowledgments

FUNDING

This work was supported by National Institutes of Health (NIH) grants ES10167 and Seahorse Biosciences (to V.D.U.), HL079364 (to J.C.C.), and HL67464 (to J.C.C.), and NIH training grants T32 HL07457 (B.G.H.) and T32 HL007918 (B.P.D.).

The abbreviations used are

NRVM	neonatal rat ventricular myocytes
XF	extracellular flux
OCR	oxygen consumption rate
ECAR	extracellular acidification rate
PPR	proton production rate
HNE	4-hydroxy-trans-2-nonenal
ECL	enhanced chemiluminescence
GSH	glutathione
ROS	reactive oxygen species
FCCP	carbonyl cyanide p-[trifluoromethoxy]-phenyl-hydrazone
MTT	3-(4,5-dimethylthiazol-2-yl)-2,5-diphenyltetrazolium bromide
HEPES	4-(2-hydroxyethyl)-1-piperazineethanesulfonic acid
NP-40	noniodet P-40
SDS	sodium dodecyl sulfate
PVDF	polyvinylidene fluoride
DMEM	Dulbecco’s Modified Eagle Medium
HRP	horseradish peroxidase
NMR	nuclear magnetic resonance
DMSO	dimethylsulfoxide
FBS	fetal bovine serum

References

1. Kingsley-Hickman PB, Sako EY, Ugurbil K, From AH, Foker JE. 31P NMR measurement of mitochondrial uncoupling in isolated rat hearts. J Biol Chem 1990;265:1545–1550. [PubMed: 2136855]
2. Gong G, Liu J, Liang P, Guo T, Hu Q, Ochiai K, Hou M, Ye Y, Wu X, Mansoor A, From AH, Ugurbil K, Bache RJ, Zhang J. Oxidative capacity in failing hearts. Am J Physiol Heart Circ Physiol 2003;285:H541–548. [PubMed: 12714322]
3. Lucas DT, Szweda LI. Declines in mitochondrial respiration during cardiac reperfusion: age-dependent inactivation of alpha-ketoglutarate dehydrogenase. Proc Natl Acad Sci USA 1999;96:6689–6693. [PubMed: 10359773]
4. Almsherqi ZA, McLachlan CS, Slocinska MB, Sluse FE, Navet R, Kocherginsky N, Kostetski I, Shi DY, Liu SL, Mossop P, Deng Y. Reduced cardiac output is associated with decreased mitochondrial efficiency in the non-ischemic ventricular wall of the acute myocardial-infarcted dog. Cell Res 2006;16:297–305. [PubMed: 16541128]

5. Petrosillo G, Ruggiero FM, Di Venosa N, Paradies G. Decreased complex III activity in mitochondria isolated from rat heart subjected to ischemia and reperfusion: role of reactive oxygen species and cardiolipin. FASEB J 2003;17:714–716. [PubMed: 12586737]
6. Paradies G, Petrosillo G, Pistolese M, Di Venosa N, Federici A, Ruggiero FM. Decrease in mitochondrial complex I activity in ischemic/reperfused rat heart: involvement of reactive oxygen species and cardiolipin. Circ Res 2004;94:53–59. [PubMed: 14656928]
7. Chen Z, Siu B, Ho YS, Vincent R, Chua CC, Hamdy RC, Chua BH. Overexpression of MnSOD protects against myocardial ischemia/reperfusion injury in transgenic mice. J Mol Cell Cardiol 1998;30:2281–2289. [PubMed: 9925365]
8. Li G, Chen Y, Saari JT, Kang YJ. Catalase-overexpressing transgenic mouse heart is resistant to ischemia-reperfusion injury. Am J Physiol 1997;273:H1090–H1095. [PubMed: 9321793]
9. Chen EP, Bittner HB, Davis RD, Folz RJ, Van Trigt P. Extracellular superoxide dismutase transgene overexpression preserves postischemic myocardial function in isolated murine hearts. Circulation 1996;94:II412–II417. [PubMed: 8901783]
10. Yoshida T, Watanabe M, Engelman DT, Engelman RM, Schley JA, Maulik N, Ho YS, Oberley TD, Das DK. Transgenic mice overexpressing glutathione peroxidase are resistant to myocardial ischemia reperfusion injury. J Mol Cell Cardiol 1996;28:1759–1767. [PubMed: 8877785]
11. Asimakis GK, Lick S, Patterson C. Postischemic recovery of contractile function is impaired in SOD2 (+/−) but not SOD1(+/−) mouse hearts. Circulation 2002;105:981–986. [PubMed: 11864929]
12. Yoshida T, Maulik N, Engelman RM, Ho YS, Magnenat JL, Rousou JA, Flack JE III, Deaton D, Das DK. Glutathione peroxidase knockout mice are susceptible to myocardial ischemia reperfusion injury. Circulation 1997;96:II–20. [PubMed: 9386101]
13. Yoshida T, Maulik N, Engelman RM, Ho YS, Das DK. Targeted disruption of the mouse Sod I gene makes the hearts vulnerable to ischemic reperfusion injury. Circ Res 2000;86:264–269. [PubMed: 10679476]
14. Strauer BE. Cardiac energetics in clinical heart disease. Basic Res Cardiol 1987;82(Suppl 2):389–402. [PubMed: 2959264]
15. Gunning JF, Coleman HN 3rd. Myocardial oxygen consumption during experimental hypertrophy and congestive heart failure. J Mol Cell Cardiol 1973;5:25–38. [PubMed: 4266588]
16. Gunning JF, Cooper Gt, Harrison CE, Coleman HN 3rd. Myocardial oxygen consumption in experimental hypertrophy and congestive heart failure due to pressure overload. Am J Cardiol 1973;32:427–436. [PubMed: 4269699]
17. Smith DR, Stone D, Darley-Usmar VM. Stimulation of mitochondrial oxygen consumption in isolated cardiomyocytes after hypoxia-reoxygenation. Free Radic Res 1996;24:159–166. [PubMed: 8728117]
18. Sako EY, Kingsley-Hickman PB, From AH, Foker JE, Ugurbil K. ATP synthesis kinetics and mitochondrial function in the postischemic myocardium as studied by 31P NMR. J Biol Chem 1988;263:10600–10607. [PubMed: 3392029]
19. Hill BG, Awe SO, Vladykovskaya E, Ahmed Y, Liu SQ, Bhatnagar A, Srivastava S. Myocardial ischaemia inhibits mitochondrial metabolism of 4-hydroxy-trans-2-nonenal. Biochem J 2009;417:513–524. [PubMed: 18800966]
20. Eaton P, Li JM, Hearse DJ, Shattock MJ. Formation of 4-hydroxy-2-nonenal-modified proteins in ischemic rat heart. Am J Physiol 1999;276:H935–H943. [PubMed: 10070077]
21. Nakamura K, Kusano K, Nakamura Y, Kakishita M, Ohta K, Nagase S, Yamamoto M, Miyaji K, Saito H, Morita H, Emori T, Matsubara H, Toyokuni S, Ohe T. Carvedilol decreases elevated oxidative stress in human failing myocardium. Circulation 2002;105:2867–2871. [PubMed: 12070115]
22. Srivastava S, Chandrasekar B, Bhatnagar A, Prabhu SD. Lipid peroxidation-derived aldehydes and oxidative stress in the failing heart: role of aldose reductase. Am J Physiol Heart Circ Physiol 2002;283:H2612–H2619. [PubMed: 12388223]
23. Esterbauer H, Schaur RJ, Zollner H. Chemistry and biochemistry of 4-hydroxynonenal, malonaldehyde and related aldehydes. Free Radic Biol Med 1991;11:81–128. [PubMed: 1937131]
24. Echtay KS, Esteves TC, Pakay JL, Jekabsons MB, Lambert AJ, Portero-Otin M, Pamplona R, Vidal-Puig AJ, Wang S, Roebuck SJ, Brand MD. A signalling role for 4-hydroxy-2-nonenal in regulation of mitochondrial uncoupling. EMBO J 2003;22:4103–4110. [PubMed: 12912909]

25. Humphries KM, Yoo Y, Szweda LI. Inhibition of NADH-linked mitochondrial respiration by 4-hydroxy-2-nonenal. Biochemistry 1998;37:552–557. [PubMed: 9425076]
26. Humphries KM, Szweda LI. Selective inactivation of alpha-ketoglutarate dehydrogenase and pyruvate dehydrogenase: reaction of lipoic acid with 4-hydroxy-2-nonenal. Biochemistry 1998;37:15835–15841. [PubMed: 9843389]
27. Lashin OM, Szweda PA, Szweda LI, Romani AM. Decreased complex II respiration and HNE-modified SDH subunit in diabetic heart. Free Radic Biol Med 2006;40:886–896. [PubMed: 16520240]
28. Benderdour M, Charron G, Deblois D, Comte B, Des RC. Cardiac mitochondrial NADP+-isocitrate dehydrogenase is inactivated through 4-hydroxynonenal adduct formation: an event that precedes hypertrophy development. J Biol Chem 2003;278:45154–45159. [PubMed: 12960146]
29. Choksi KB, Boylston WH, Rabek JP, Widger WR, Papaconstantinou J. Oxidatively damaged proteins of heart mitochondrial electron transport complexes. Biochim Biophys Acta 2004;1688:95–101. [PubMed: 14990339]
30. Chen J, Henderson GI, Freeman GL. Role of 4-hydroxynonenal in modification of cytochrome c oxidase in ischemia/reperfused rat heart. J Mol Cell Cardiol 2001;33:1919–1927. [PubMed: 11708837]
31. Ji C, Amarnath V, Pietenpol JA, Marnett LJ. 4-hydroxynonenal induces apoptosis via caspase-3 activation and cytochrome c release. Chem Res Toxicol 2001;14:1090–1096. [PubMed: 11511183]
32. Vieira HL, Belzacq AS, Haouzi D, Bernassola F, Cohen I, Jacotot E, Ferri KF, El Hamel C, Bartle LM, Melino G, Brenner C, Goldmacher V, Kroemer G. The adenine nucleotide translocator: a target of nitric oxide, peroxynitrite, and 4-hydroxynonenal. Oncogene 2001;20:4305–4316. [PubMed: 11466611]
33. Chen CH, Budas GR, Churchill EN, Disatnik MH, Hurley TD, Mochly-Rosen D. Activation of aldehyde dehydrogenase-2 reduces ischemic damage to the heart. Science 2008;321:1493–1495. [PubMed: 18787169]
34. Churchill EN, Disatnik MH, Mochly-Rosen D. Time-dependent and ethanol-induced cardiac protection from ischemia mediated by mitochondrial translocation of varepsilonPKC and activation of aldehyde dehydrogenase 2. J Mol Cell Cardiol 2009;46:278–284. [PubMed: 18983847]
35. Champattanachai V, Marchase RB, Chatham JC. Glucosamine protects neonatal cardiomyocytes from ischemia-reperfusion injury via increased protein O-GlcNAc and increased mitochondrial Bcl-2. Am J Physiol Cell Physiol 2008;294:C1509–1520. [PubMed: 18367586]
36. Ferrick DA, Neilson A, Beeson C. Advances in measuring cellular bioenergetics using extracellular flux. Drug Discov Today 2008;13:268–274. [PubMed: 18342804]
37. Hill BG, Haberzettl P, Ahmed Y, Srivastava S, Bhatnagar A. Unsaturated lipid peroxidation-derived aldehydes activate autophagy in vascular smooth-muscle cells. Biochem J 2008;410:525–534. [PubMed: 18052926]
38. Oh JY, Giles N, Landar A, Darley-Usmar V. Accumulation of 15-deoxy-delta(12,14)-prostaglandin J2 adduct formation with Keap1 over time: effects on potency for intracellular antioxidant defence induction. Biochem J 2008;411:297–306. [PubMed: 18237271]
39. Mosmann T. Rapid colorimetric assay for cellular growth and survival: application to proliferation and cytotoxicity assays. J Immunol Methods 1983;65:55–63. [PubMed: 6606682]
40. Nakamura K, Kusano KF, Matsubara H, Nakamura Y, Miura A, Nishii N, Banba K, Nagase S, Miyaji K, Morita H, Saito H, Emori T, Ohe T. Relationship between oxidative stress and systolic dysfunction in patients with hypertrophic cardiomyopathy. J Card Fail 2005;11:117–123. [PubMed: 15732031]
41. Mak S, Lehotay DC, Yazdanpanah M, Azevedo ER, Liu PP, Newton GE. Unsaturated aldehydes including 4-OH-nonenal are elevated in patients with congestive heart failure. J Card Fail 2000;6:108–114. [PubMed: 10908084]
42. Srivastava S, Chandra A, Wang LF, Seifert WE Jr, DaGue BB, Ansari NH, Srivastava SK, Bhatnagar A. Metabolism of the lipid peroxidation product, 4-hydroxy-trans-2-nonenal, in isolated perfused rat heart. J Biol Chem 1998;273:10893–10900. [PubMed: 9556565]
43. Wu M, Neilson A, Swift AL, Moran R, Tamagnine J, Parslow D, Armistead S, Lemire K, Orrell J, Teich J, Chomicz S, Ferrick DA. Multiparameter metabolic analysis reveals a close link between

attenuated mitochondrial bioenergetic function and enhanced glycolysis dependency in human tumor cells. Am J Physiol Cell Physiol 2007;292:C125–136. [PubMed: 16971499]

44. David H, Meyer R, Marx I, Guski H, Wenzelides K. Morphometric characterization of left ventricular myocardial cells of male rats during postnatal development. J Mol Cell Cardiol 1979;11:631–638. [PubMed: 480364]
45. Schaper J, Meiser E, Stammler G. Ultrastructural morphometric analysis of myocardium from dogs, rats, hamsters, mice, and from human hearts. Circ Res 1985;56:377–391. [PubMed: 3882260]
46. Giordano FJ. Oxygen, oxidative stress, hypoxia, and heart failure. J Clin Invest 2005;115:500–508. [PubMed: 15765131]
47. Katz AM. Changing strategies in the management of heart failure. J Am Coll Cardiol 1989;13:513–523. [PubMed: 2645340]
48. Boudina S, Sena S, O'Neill BT, Tathireddy P, Young ME, Abel ED. Reduced mitochondrial oxidative capacity and increased mitochondrial uncoupling impair myocardial energetics in obesity. Circulation 2005;112:2686–2695. [PubMed: 16246967]
49. Veronneau M, Comte B, Des RC. Quantitative gas chromatographic-mass spectrometric assay of 4-hydroxynonenal bound to thiol proteins in ischemic/reperfused rat hearts. Free Radic Biol Med 2002;33:1380–1388. [PubMed: 12419470]
50. Fiorillo C, Nediani C, Ponziani V, Giannini L, Celli A, Nassi N, Formigli L, Perna AM, Nassi P. Cardiac volume overload rapidly induces oxidative stress-mediated myocyte apoptosis and hypertrophy. Biochim Biophys Acta 2005;1741:173–182. [PubMed: 15894467]
51. Srivastava S, Chandrasekar B, Gu Y, Luo J, Hamid T, Hill BG, Prabhu SD. Downregulation of CuZn-superoxide dismutase contributes to beta-adrenergic receptor-mediated oxidative stress in the heart. Cardiovasc Res 2007;74:445–455. [PubMed: 17362897]
52. Luo J, Hill BG, Gu Y, Cai J, Srivastava S, Bhatnagar A, Prabhu SD. Mechanisms of Acrolein-Induced Myocardial Dysfunction: Implications for Environmental and Endogenous Aldehyde Exposure. Am J Physiol Heart Circ Physiol 2007;293:H3673–H3684. [PubMed: 17921335]
53. Irwin WA, Gaspers LD, Thomas JA. Inhibition of the mitochondrial permeability transition by aldehydes. Biochem Biophys Res Commun 2002;291:215–219. [PubMed: 11846392]
54. Parker N, Vidal-Puig A, Brand MD. Stimulation of mitochondrial proton conductance by hydroxynonenal requires a high membrane potential. Biosci Rep 2008;28:83–88. [PubMed: 18384278]
55. Nicholls DG, Johnson-Cadwell L, Vesce S, Jekabsons M, Yadava N. Bioenergetics of mitochondria in cultured neurons and their role in glutamate excitotoxicity. J Neurosci Res 2007;85:3206–3212. [PubMed: 17455297]
56. Yadava N, Nicholls DG. Spare respiratory capacity rather than oxidative stress regulates glutamate excitotoxicity after partial respiratory inhibition of mitochondrial complex I with rotenone. J Neurosci 2007;27:7310–7317. [PubMed: 17611283]
57. Choi SW, Gerencser AA, Nicholls DG. Bioenergetic analysis of isolated cerebrocortical nerve terminals on a microgram scale: spare respiratory capacity and stochastic mitochondrial failure. J Neurochem 2009;109:1179–1191. [PubMed: 19519782]

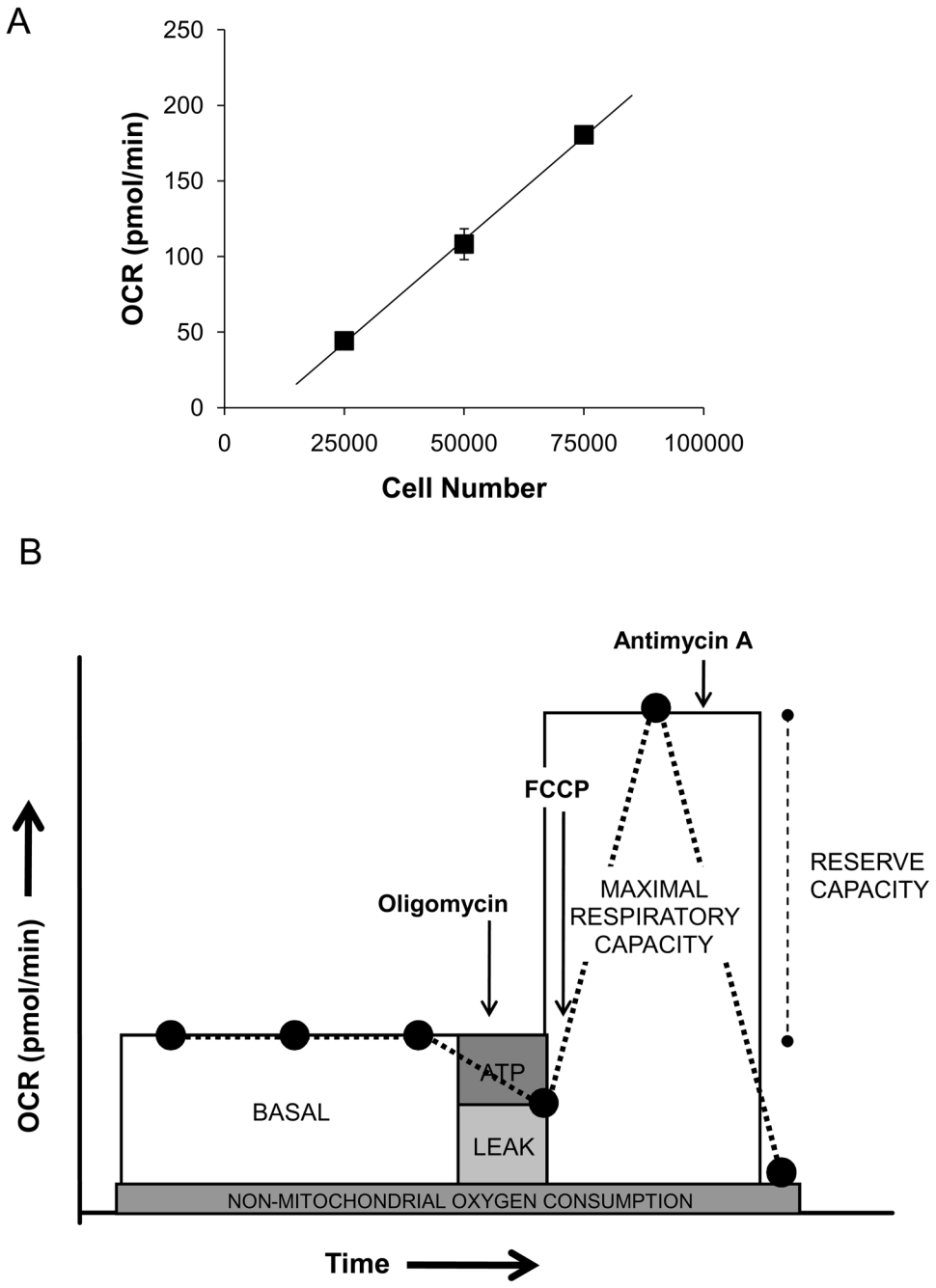

Figure 1. Measurement of bioenergetic parameters in myocytes using extracellular flux technology

Oxygen consumption rate (OCR) from isolated neonatal rat ventricular myocytes (NRVM): (**A**) NRVM were seeded at 25,000–75,000 cells/well and the oxygen consumption rate (OCR) was measured. y=0.0027x – 25.244, R^2 = 0.99. (**B**) *In situ* mitochondrial function assay: After three baseline OCR measurements, oligomycin (1 μg/ml), FCCP (1 μM), and antimycin A (10 μM) are injected sequentially with OCR measurements recorded after each injection. ATP-linked oxygen consumption (ATP) and the OCR due to proton leak (leak) can be calculated using the basal and the oligomycin-sensitive rate. Injection of the uncoupling agent, FCCP, is then used to determine the maximal respiratory capacity. Lastly, injection of antimycin A allows for the measurement of non-mitochondrial oxygen consumption. The reserve capacity

is calculated by subtracting the maximal rate of oxygen consumption by the pre-oligomycin rate.

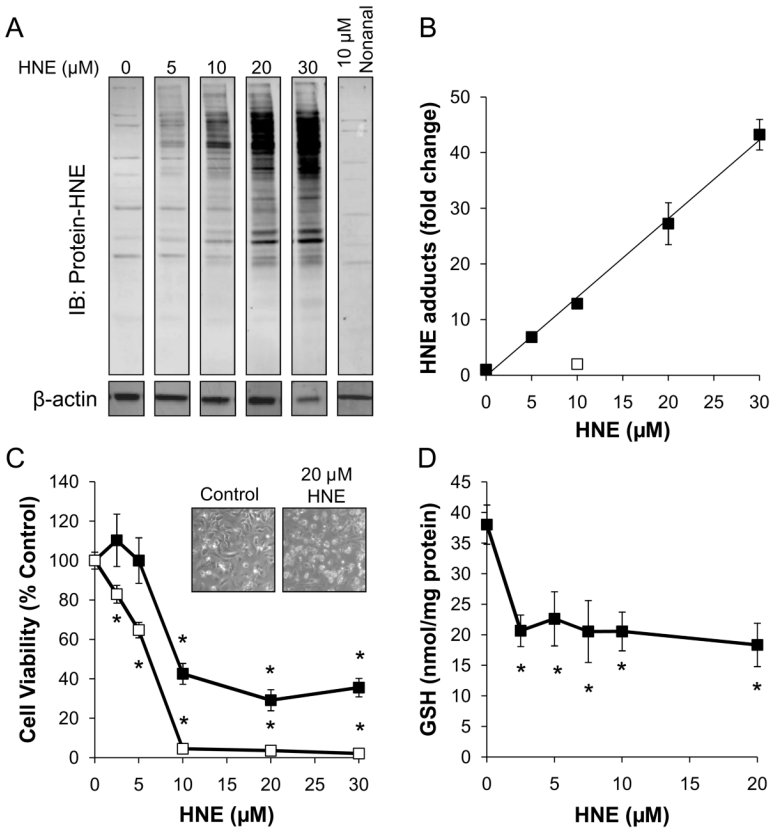

Figure 2. HNE promotes protein damage and myocyte cell death

NRVM were treated with the indicated concentrations of HNE or nonanal for 90 min for measurement of protein-HNE adducts or for 8 and 16 h for cell death assay. (**A**) Western blots of HNE-modified proteins: After treatment with the indicated concentrations of HNE, myocytes were lysed, and protein-HNE adducts were detected by immunoblotting. Actin was used as a normalization control for Western blotting experiments, and nonanal was used as a non-electrophilic analog control for HNE. (**B**) Relative quantification of protein-HNE modifications: Protein-HNE antibody immunoreactivity was quantified by densitometry, and the fold change of immunoreactivity over non-treated cells was plotted as a function of HNE concentration; y=1.4127x – 0.1261, R^2=0.99. (**C**) Cell death assay of HNE-treated myocytes: NRVM were exposed to 0–30 μM HNE for 8h (■) and 16h (□), followed by measurement of cell death by MTT assay. The inset shows the micrograph of the control and HNE treated cells (magnification 10 x). **D**) Total GSH content was measured in NRVM cell lysates exposed to 0–20μM HNE for 90 min. Data are expressed as the nmol GSH/mg protein. All data shown are means ± sem, n≥3; *p<0.01 vs. non-HNE treated myocytes from each time point.

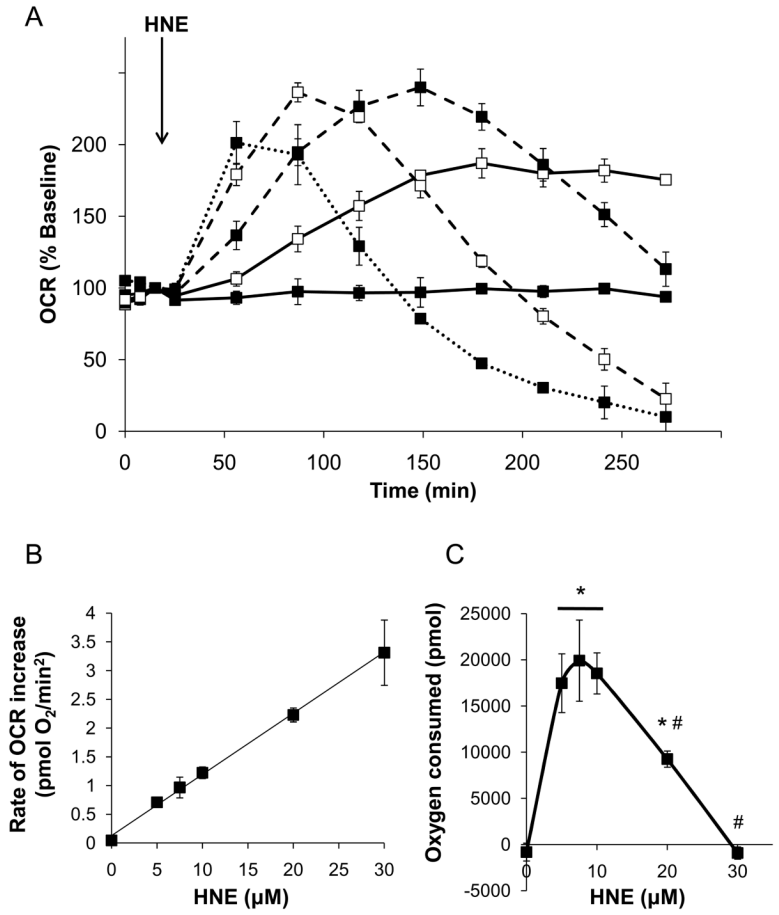

Figure 3. HNE increases oxygen consumption in isolated myocytes

Oxygen consumption rate (OCR) plots from myocytes exposed to 0–30 μM HNE: (**A**) The basal OCR was measured followed by addition of 0 (filled squares, solid line), 5 (open squares, solid line), 10 (filled squares, dashed line), 20 (open squares, dashed line, and 30 μM HNE (closed squares, dotted line), as indicated by the arrow. The rate of oxygen consumption was then measured for the indicated time. The OCR values are shown as the percent of baseline for each group. For visual clarity, statistical indicators were omitted from the graph. (**B**) The slope of the initial increase in OCR due to HNE treatment was then measured and plotted as the rate of OCR increase; $y=0.1065x + 0.1283$, $R^2=0.99$. (**C**) Area under the curve analyses were used to determine the overall amount of oxygen consumed with each treatment. In panels A–C, data shown are means ± SEM, n≥3. *p<0.05 vs. cells not treated with HNE; #p<0.05 vs. cells treated with 5–10 μM HNE.

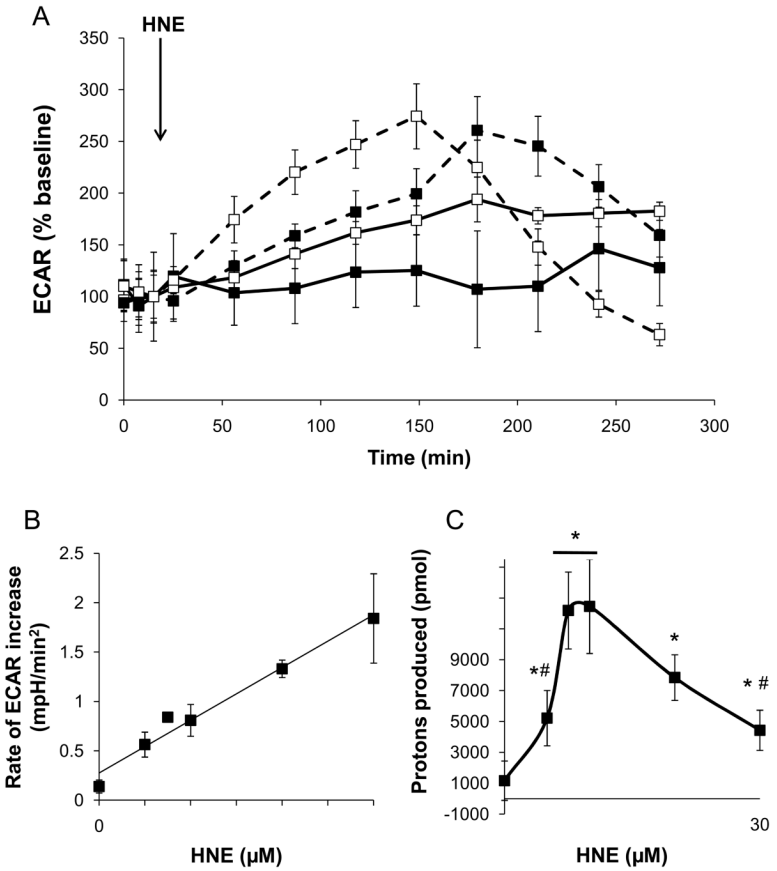

Figure 4. HNE increases glycolytic rate in isolated myocytes

Measurements of proton production from myocytes exposed to 0–30 μM HNE: (A) The basal extracellular acidification rate (ECAR) was measured followed by addition of 0 (filled squares, solid line), 5 (open squares, solid line), 10 (filled squares, dashed line), and 20 μM HNE (open squares, dashed line), as indicated by the arrow. The rates of extracellular acidification, indicative of changes in glycolytic flux, were then measured for the indicated time. For visual clarity, the 30 μM HNE group and statistical indicators were omitted from the graph. (**B**) The slope of the initial increase in ECAR due to HNE treatment was then measured and plotted as the rate of ECAR increase; $y=0.0534x + 0.2751$, $R^2=0.97$. (**C**) Area under the curve analyses of the proton production rate were used to determine the overall amount of protons produced with each treatment. In panels A–C, data shown are means ± SEM, n≥3. *p<0.05 vs. cells not treated with HNE; #p<0.05 vs. cells treated with 7.5 and 10 μM HNE.

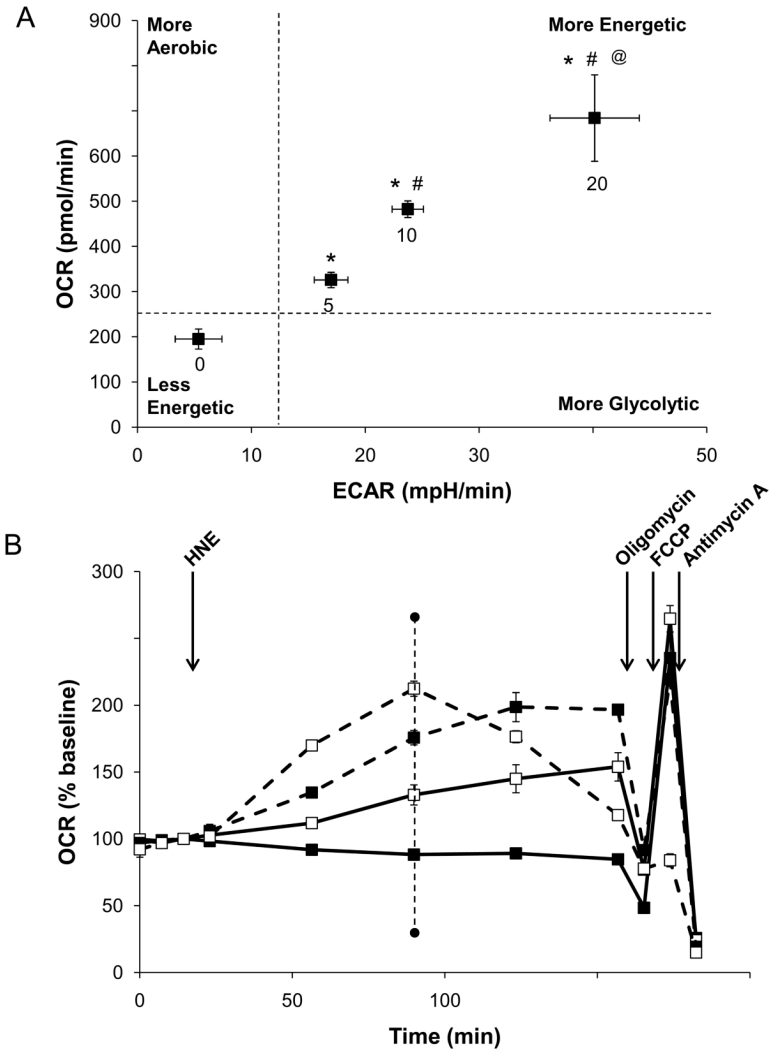

Figure 5. Changes in the mitochondrial and glycolytic profiles due to HNE treatment

(**A**) Metabolic profile of the stimulatory effect of HNE on aerobic and anaerobic respiration: The OCR and ECAR were plotted against one another at the time where OCR was increased to the greatest extent in cells treated with 20 μM HNE (from experiment in panel B – dotted line at ~80 min timepoint). (**B**) After measurement of the basal OCR, HNE was injected to 0 (filled squares, solid line), 5 (open squares, solid line), 10 (filled squares, dashed line), and 20 μM (open squares, dashed line) final concentrations as indicated. Mitochondrial function assay was then performed by sequential injections of oligomycin, FCCP, and antimycin A to determine the level of proton leak and ATP-linked oxygen consumption, the maximal OCR, and the non-mitochondrial OCR, respectively. Data in panels A and B are means ± SEM, n≥3. *p<0.05 vs. cells not treated with HNE; $^{\#}$p<0.05 vs. cells treated with 5 μM HNE; $^{@}$p<0.05 vs. cells treated with 5–10 μM HNE.

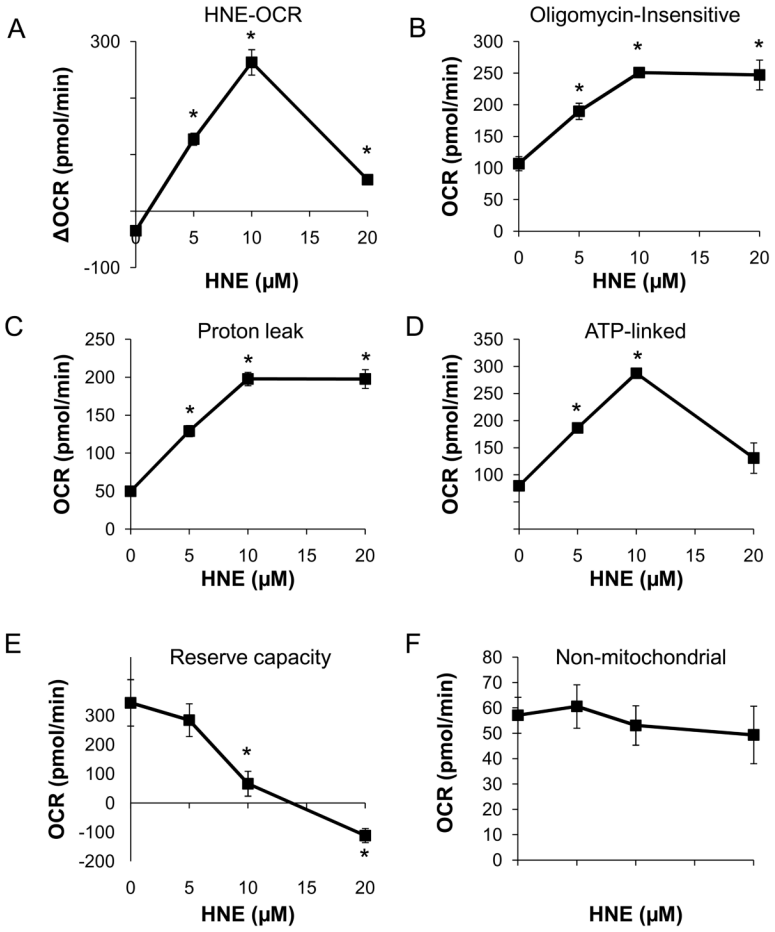

Figure 6. Specific defects in mitochondrial function caused by HNE

The HNE-induced changes in the following parameters derived from the data in Figure 5 are shown: (**A**) The HNE–dependent change in OCR relative to the initial basal OCR assessed immediately before the addition of oligomycin (**B**) the HNE-dependent change in the Oligomycin-insensitive OCR (**C**) The OCR ascribed to proton leak (**D**) The OCR ascribed to ATP-synthesis (**E**) bioenergetic reserve capacity, and (**F**) the non-mitochondrial OCR. Data represent means ± SEM. N ≥ 3/group. *$p<0.05$ vs. myocytes not treated with HNE.